Beach Profiling and LIDAR Bathymetry: An Overview with Case Studies

Author(s) :Victor Klemas
Source: Journal of Coastal Research, 27(6):1019-1028. 2011.
Published By: Coastal Education and Research Foundation
DOI:
URL: http://www.bioone.org/doi/full/10.2112/JCOASTRES-D-11-00017.1

Journal of Coastal Research	27	6	1019–1028	West Palm Beach, Florida	November 2011

Beach Profiling and LIDAR Bathymetry: An Overview with Case Studies

Victor Klemas

College of Earth,
Ocean and Environment
University of Delaware
Newark, DE 19716, U.S.A.

www.cerf-jcr.org

www.JCRonline.org

ABSTRACT

KLEMAS, V., 2011. Beach profiling and LIDAR bathymetry: an overview with case studies. *Journal of Coastal Research,* 27(6), 1019–1028. West Palm Beach (Florida), ISSN 0749-0208.

Light detection and ranging (LIDAR) techniques, combined with Global Positioning Systems (GPSs), make it possible to obtain accurate topographical and bathymetric maps, including maps of shoreline positions. LIDAR surveys can produce 10- to 15-cm vertical accuracy at a spatial resolution greater than one elevation measurement *per* square meter. This meets the requirements of many coastal research and management applications of LIDAR, including flood zone delineation, monitoring beach-nourishment projects, and mapping changes along sandy coasts and shallow benthic environments from storms or long-term sedimentary processes. Typically, a LIDAR sensor may collect data down to depths of about three times the Secchi depth. If the depth or the water turbidity is too great, acoustic echo-sounding is used. Airborne LIDARs have also been applied with hyperspectral imagers to map wetlands, beaches, coral reefs, and submerged aquatic vegetation (SAV). The objective of this article is to review the use of LIDAR techniques for collecting topographic and bathymetric data and to present three case studies, including lessons learned from each.

ADDITIONAL INDEX WORDS: *LIDAR bathymetry, beach profiling, coastline delineation, coastal geomorphology, flood zone delineation, sea level rise.*

INTRODUCTION AND BACKGROUND

Information on beach profiles and coastal bathymetry is important for studies of near-shore geomorphology, hydrology, and sedimentary processes. To plan sustainable coastal development and implement effective beach erosion control, flood zone delineation, and ecosystem protection, coastal managers and scientists need information on long-term and short-term changes taking place along the coast, including changes in beach profiles from erosion by storms and littoral drift, wetlands changes from inundation, *etc*. (Gesch, 2009; West, Lillycrop, and Pope, 2001).

Before the advent of the Global Positioning System (GPS) and Light Detection and Ranging (LIDAR) systems, shoreline position analysis and beach profiling were based on historical aerial photographs and topographical maps (Jensen, 2007; Morton and Miller, 2005). For instance, to map long-term changes of the shoreline from beach erosion, time series of historical, aerial photographs were used in the past (Rasher and Weaver, 1990).

Topographical and depth data can now be effectively acquired at various spatial scales by airborne laser surveys using LIDAR techniques (Ackermann, 1999; Guenther, Tomas, and LaRocque, 1996; Krabill *et al.,* 2000; Lillycrop, Pope, and Wozencraft, 2002). A laser transmitter/receiver mounted on an aircraft transmits a laser pulse that travels to the land surface or the air–water interface, and a portion of that energy reflects back to the receiver. The land topography is obtained from the LIDAR-pulse travel time. On water, some of the energy propagates through the water column and reflects off the sea bottom. The water depth is calculated from the time lapse between the surface return and the bottom return (Hapke, 2010; Purkis and Klemas, 2011).

The objective of this article is to review the use of LIDAR techniques for collecting topographical and bathymetric data and to present three case studies. Based on the case studies, lessons learned and recommendations for users are provided.

BEACH PROFILING AND SHORELINE DELINEATION

Beach profiles and shoreline positions can change rapidly with the seasons and after storms, in addition to exhibiting slower changes due to littoral drift and sea level rise (Stockdon, Doran, and Sallenger, 2009). As shown in the Figure 1, during winter storms, waves remove sand from the beach and deposit it offshore, typically in bar formations. During summer, milder wave formations move the bars onshore and rebuild the wider berm for the "summer beach." Long-term changes of shorelines from littoral drift or sea-level rise can be aggravated by artificial structures, such as jetties, seawalls, and groins (Finkl, 1996; Irish and White, 1998; Klemas, 2009; Wang, 2010).

To map long-term changes of the shoreline from beach erosion, a time series of historical, aerial photographs and

DOI: 10.2112/JCOASTRES-D-11-00017.1 received 13 January 2011; accepted in revision 20 February 2011.
Published Pre-print online 9 June 2011.

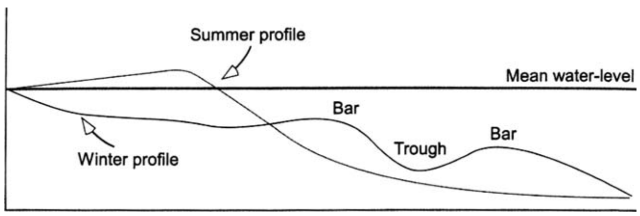

Figure 1. Changes in beach profiles between summer and winter caused by changes in wave climate. During winter storms, the beach is eroded and seaward cross-shore sediment transport results in the formation of offshore bars (Purkis and Klemas, 2011).

topographic maps can be used. Aerial photographs are available dating back to the 1930s, and topographic maps exist to extend the record of shoreline change to the mid to late 1800s. Such data are held by local, state, and federal agencies, including the U.S. Geological Survey and the U.S. Department of Agriculture's Soil Conservation Service. These organizations also have various types of maps, including planimetric, topographic, quadrangle, thematic, ortho-photo, satellite, and digital maps (Jensen, 2007; Purkis and Klemas, 2011; Rasher and Weaver, 1990).

One way of performing a shoreline position analysis is to divide the shoreline into segments that are eroding or accreting uniformly. The change in the distance of the waterline is then measured in reference to some stable feature, such as a coastal highway. Because the instantaneous waterline in the image is not a temporally representative shoreline, the high-water line, also referred to as the wet/dry line, has been a commonly used indicator that is visible in most images. Other indicators include the vegetation line, the bluff line or constructed shore accoutrements (Boak and Turner, 2005; Thieler and Danforth, 1994). Some practical, direct field methods are also available and are described in the literature (Andrade and Ferreira, 2006).

More recently, GPSs, combined with LIDAR techniques, make it possible to obtain accurate topographical maps, including shoreline positions. Airborne LIDAR surveying has been significantly enhanced by kinematic differential GPS methods, which enable the positioning of small aircraft to within several centimeters. Inertial navigation systems provide three-dimensional aircraft orientation making aerotriangulation with ground data points unnecessary. LIDAR transmitters can provide elevation measurements at 1000 soundings *per* second with ground resolutions of 2 to 4 meters and vertical accuracies of 10 to 15 cm (Brock and Sallenger, 2000; Cracknell and Hayes, 2007; Finkl, Benedet, and Andrews, 2005; Hapke, 2010).

Such performance is important for various coastal research applications of LIDAR, including flood-zone delineation, monitoring beach-nourishment projects, and mapping changes along barrier island beaches and other sandy coasts (Brock and Purkis, 2009; Deronde *et al.,* 2005; Gares, Wang and White, 2007; Raber *et al.,* 2007; Webster *et al.,* 2004; Wozencraft and Millar, 2005). The ability of LIDAR to rapidly survey long, narrow strips of terrain is very valuable because beaches are elongate, highly dynamic, sedimentary environments that undergo seasonal and long-term erosion or accretion and are affected by severe storms (Kempeneers *et al.,* 2009; Stockdon *et al.,* 2002; Zhou, 2010).

A typical beach-profiling procedure using LIDAR may include cross-shore profiles every 10 m. Beach slope and location and elevation of the berm, dune base, and dune crest can be determined from these beach profiles. One can use a known vertical datum to remove the subjective nature of identifying the shoreline. The waterline is then readily identified because laser returns from the sea are noisy. All points that lie seaward of that line are deleted from the profile. A vertical range around the elevation datum is then chosen (*e.g.,* 1.0 m), and all points that do not fall within that range are removed from the profile. Finally, a linear regression is fit through the cluster of points to produce the horizontal position of the shoreline and the slope, using the elevation datum and regression analysis (Stockdon *et al.,* 2002).

A LIDAR aircraft-mapping configuration usually includes a light aircraft equipped with a LIDAR instrument and GPS, which is operated in tandem with a GPS base station (Figure 2). In coastal applications, the aircraft flies along the coast at heights of about 300–1000 m, surveying a ground swath directly below the aircraft. The aircraft position throughout the flight is recorded by an onboard GPS receiver. The aircraft GPS signals are later combined with signals concurrently collected by a nearby GPS base station. Differential-kinematic GPS postprocessing determines the aircraft flight trajectory to within about 5 cm (Brock and Sallenger, 2000; Cracknell and Hayes, 2007; Irish and Lillycrop, 1999; Wang, 2010). Although airborne laser mapping may be carried out at night, flight safety dictates that coastal LIDAR operations are normally confined to daylight hours and timed to coincide with low tide to maximize coverage of the beach face.

BATHYMETRIC TECHNIQUES

Remote-sensing techniques that have been used to map coastal water depth include multispectral imaging, photogrammetric (stereoscopic) imaging, and LIDAR depth-sounding. The photogrammetric imaging technique is not very effective in coastal waters because the water column and its turbidity may distort the bottom image and make the stereo analysis difficult. The multispectral imaging approach depends on different visible wavelengths penetrating to different depths. It has not been very accurate until the recent physics-based approach developed by Lee *et al.* (2010). Acoustic systems, such as echo-sounding profilers, multibeam echo-sounders, and side-scan sonars, are operated from ships and submerged vehicles to measure depths and map bottom features, especially in deep or turbid waters (Coasta, Battista, and Pittman, 2009; Mayer *et al.,* 2007; Pittenger, 1989; Wilson *et al.,* 2007). Because LIDAR and acoustic depth sounding are the two most reliable techniques, they will be emphasized in this article.

In LIDAR bathymetry, a laser transmitter/receiver mounted on an aircraft transmits a pulse that travels to the air–water interface, and a portion of that energy reflects back to the receiver. The remaining energy propagates through the water column and reflects off the sea bottom. Because the velocity of the light pulse is known, the water depth can be calculated from

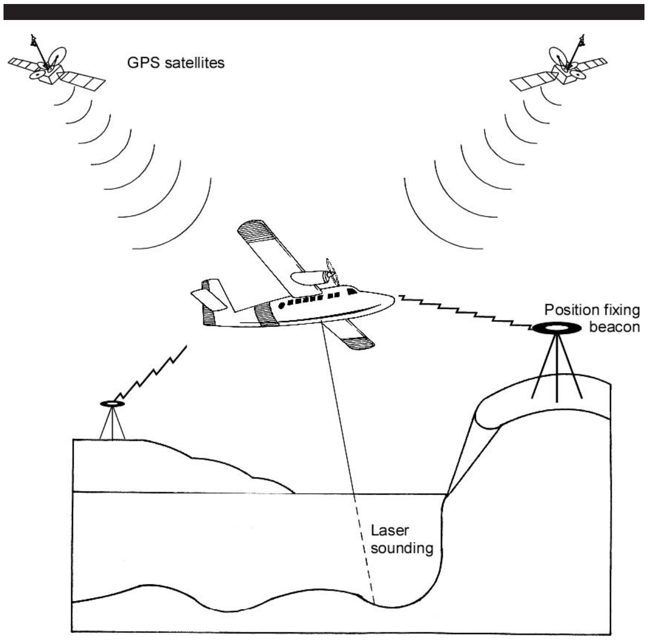

Figure 2. Configuration for a LIDAR topography operation (modified from Muirhead and Cracknell, 1986).

the time lapse between the surface return and the bottom return. Each sounding is corrected for water-level fluctuations, using either vertical aircraft positioning from GPS or by referencing the LIDAR measurements of water surface location with water-level gauge measurements. Because laser energy is lost to refraction, scattering, and absorption at the water surface, the sea bottom and inside the water column, these effects limit the strength of the bottom return and limit the maximum detectable depth.

Examples of LIDAR applications include regional mapping of changes along sandy coasts from storms or long-term sedimentary processes and the analysis of shallow benthic environments (Bonisteel *et al.,* 2009a; Guenther, Tomas, and LaRocque, 1996; Gutierrez *et al.,* 1998; Irish and Lillycrop, 1997; Kempeneers *et al.,* 2009; Sallenger *et al.,* 1999). In the coastal zone, there is considerable utility in being able to capture seamlessly and simultaneously topographical LIDAR above the water with bathymetric postings in the adjacent ocean. This objective is achievable but, as will be seen below, it demands the use of multiple lasers and/or advanced profiling technologies.

To maximize water penetration, bathymetric LIDARs employ a blue-green laser with a typical wavelength of 530 nm to range the distance to the seabed. With the near-exponential attenuation of electromagnetic energy by water with increasing wavelengths, a pure-blue laser with a wavelength shorter than 500 nm would offer greater penetration. However, that wavelength is not used because, first, blue light interacts much more strongly with the atmosphere than do longer wavelengths, and, second, a high-intensity blue laser is energetically less efficient than a blue-green laser and consumes a disproportionately large amount of instrument power. This, combined with blue lasers suffering from temperature problems at high powers, explains why blue-green is the preferred wavelength for bathymetric LIDAR profilers.

Conversely, terrestrial topographical LIDARs typically use near-infrared (NIR) lasers with a wavelength of 1064 nm. As is the case for the blue-green lasers used in hydrography, this NIR wavelength is focused and easily absorbed by the eye. Therefore, the maximum power of the LIDAR system is limited by the need to make them eye-safe. Although less-accurate, military instruments often use lasers with wavelengths as long as 1550 nm, which hold the dual advantage of being eye-safe at much higher power levels and the beam not being visible using night-vision goggles. Although bathymetric lasers are limited in their accuracy by water-column absorption, terrestrial infrared lasers suffer from null or poor returns from certain materials and surfaces, such as water, asphalt, tar, clouds, and fog, all of which absorb NIR wavelengths.

Because they do not penetrate water, NIR topographical lasers cannot be used to assess bathymetry. However, blue-green hydrographical lasers do reflect off terrestrial targets and can be used to measure terrain. Traditionally, their accuracy and spatial resolution has been lower than that provided by a dedicated NIR topographical instrument. Dual-wavelength LIDAR provides both bathymetric and topographical LIDAR mapping capability by carrying both an NIR and a blue-green laser. The NIR laser is not redundant over water because it reflects off the air–water interface and can be used to refine the surface position as well as to distinguish dry land from water using signal polarization (Guenther, 2007).

In addition, specific LIDAR systems, like the SHOALS, record the red wavelength Raman signal (647 nm). The Raman signal comes from interactions between the blue-green laser and water molecules, causing part of the energy to be backscattered during the change in wavelengths (Guenther, LaRocque, and Lillycrop, 1994). This is also useful for localizing the air–water interface when experiencing incorrect surface detections from land reflection or the presence of unexpected targets, such as birds. A detailed description of the SHOALS system is provided in the next section on U.S. Army Corps of Engineers (USACE) projects and by Lillycrop, Irish, and Parson (1997).

By employing a very high scan-rate, state-of-the-art systems, such as the Experimental Advanced Airborne Research LIDAR (EAARL), both topography and bathymetry can be measured from the return time of a single blue-green laser (Bonisteel *et al.,* 2009b; McKean *et al.,* 2009; Nayegandhi, Brock, and Wright, 2009). Operating in the blue-green portion of the electromagnetic spectrum, the EAARL is specifically designed to measure submerged topography and adjacent coastal land elevations seamlessly in a single scan of transmitted laser pulses. Figure 3 shows such a bathymetric–topographic digital elevation model (DEM) of a section of the Assateague Island National Seashore (Chincoteague, Virginia), captured by the EAARL. Assateague Island National Seashore consists of a 37-mile-long barrier island along the Atlantic coasts of Maryland and Virginia. This experimental advance signals a future move toward commercial implementation of dual-application but single-wavelength instruments (Krabill et al.,2000; Wozencraft and Lillycrop, 2003).

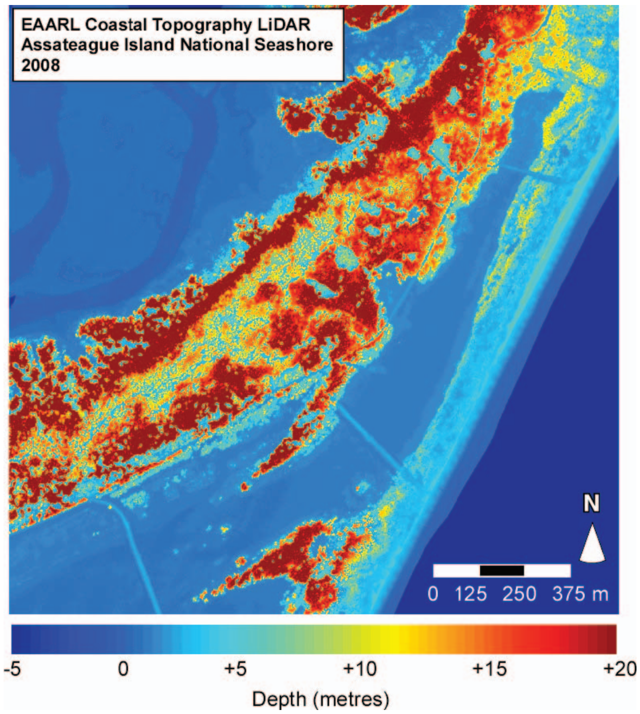

Figure 3. Coastal topography for a section of the Assateague Island National Seashore acquired using the airborne Experimental Advanced Airborne Research LIDAR (EAARL) (Bonisteel *et al.,* 2009b). Credit: USGS.

Although the EAARL and dual-wavelength LIDARs offer nearly seamless profiles between bathymetry and terrestrial terrain, neither bathymetric system can acquire dependable bathymetric data in very shallow depths or over white water in the surf zone. When whitecaps are present, the laser does not penetrate the water column. Furthermore, if the depth is less than 2 m, even in clear water, it becomes difficult to separate the laser pulse returning from the water surface from the one reflected by the bottom bed (Bonisteel *et al.,* 2009b; Parson *et al.,* 1996; Philpot, 2007). For coastal mapping, both problems are obviated by combining successive flights at low tide with a topographical LIDAR and at high tide with a bathymetric LIDAR (Pastol, Le Roux, and Louvart, 2007; Sinclair, 2008; Stoker *et al.,* 2009). Such a strategy is not possible for coastal areas that do not have large tidal variations or for nontidal, inland water bodies.

Laser depth-sounding techniques have proven most effective in clear water, where LIDAR pulses have penetrated down to 50 m. Typical flight parameters for airborne LIDARs used in bathymetry are shown in Table 1. Optical water clarity is the most limiting factor for LIDAR depth detection, so it is important to conduct the LIDAR overflights during tidal and current conditions that minimize the water turbidity due to sediment resuspension and river inflow (Sinclair, 2008).

The LIDAR system must have a kd factor large enough to accommodate the water depth and water turbidity at the study site (k = medium attenuation coefficient; d = maximum water-penetration depth). For instance, if a given LIDAR system has a $kd = 4$ and the turbid water has an attenuation coefficient of $k = 1$, the system will be effective only to depths of approximately 4 m. Typically, a LIDAR sensor may collect data down to depths of about three times the Secchi (visible) depth (Estep, Lillycrop, and Parson, 1994; Sinclair, 1999). Beyond that depth, one may have to use acoustic (sonar) echo-sounding techniques (Brock and Sallenger, 2000).

Table 1. *Typical LIDAR flight parameters (DGPS = differential GPS mode; KGPS = kinematic GPS mode).*

Flying height	300–1000 m
Vertical accuracy	±15 cm
Horizontal accuracy	DGPS = 3 m; KGPS = 1 m
Maximum depth	50 m (clear water)
Typical kd product	4
Coastal k	0.2–0.8 (d = 5–20 m)
Estuarine k	1.0–4.0 (d = 1–4 m)
Sounding density	3–15 m
Sun angle	18°–25° (to minimize glare)
Scan geometry	Circular (220-m swath)
Sea state	Low (0–1 Beaufort scale)
Water penetration	Green LIDAR (532 nm) used
Aircraft height	Infrared LIDAR (1064 nm) used

There are various sonar systems available. Echo-sounding profilers, which measure water depth and changes in bottom topography, send out pulses of acoustic energy beneath the boat or other platform. The acoustic "ping" is reflected off the bottom and off submerged objects and is recorded by the transceiver. The depth-to-target calculation is based on how long it took the reflected pulse to return to the surface and the speed of sound in water under prevailing environmental conditions. The earliest sounders used single beams, but the newer systems use multiple beams with large arrays of beams measuring bottom depths across a wide swath (Bergeron, Worley and O'Brien, 2007; Cracknell and Hayes, 2007).

Side-scan imaging sonars emit acoustic pulses in very wide, fan-shaped beams to both sides and at right angles to the tracks to produce an image of the sea bottom from the backscattered acoustic energy. Sonar echo-sounders and side-scan sonars are frequently housed in a torpedo-shaped "fish," which is towed by cable behind the survey ship at a predetermined height off the bottom (Avery and Berlin, 1992; Pittenger, 1989; Thompson and Schroeder, 2010). More recently, various acoustic sensors have been housed in Remotely Controlled Vehicles (ROVs) or Autonomous Underwater Vehicles (AUVs) (Chadwick, 2010).

Mapping submerged aquatic vegetation (SAV) and coral reefs requires high-resolution (1–4 m) imagery (Mumby and Edwards, 2002; Purkis, 2005; Trembanis, Hiller, and Patterson, 2008). Coral reef ecosystems usually exist in clear water, and their images can be classified to show different forms of coral reef, dead coral, coral rubble, algal cover, sand lagoons, and different densities of sea grasses, *etc*. However, SAVs may grow in waters that are more turbid and thus can be more difficult to map. High-resolution (*e.g.,* IKONOS earth observation satellite), multispectral imagers have been used in the past to map eelgrass and coral reefs. Hyperspectral imagers should improve the results significantly by allowing users to identify more estuarine and intertidal habitat classes (Garono *et al.,* 2004; Maeder *et al.,* 2002; Mishra *et al.,* 2006; Nayegandhi and Brock, 2009; Philpot *et al.,* 2004; Wang and Philpot, 2007).

Airborne LIDARS have also been used with multispectral or hyperspectral imagers to map coral reefs and SAV (Brock and Purkis, 2009; Brock *et al.,* 2004; Yang, 2009).

USACE MORPHOLOGY AND COASTAL-CHANGE MAPPING

Beach and surf-zone models provide some basic insight on the dynamic interaction of waves and beaches. The physical processes that shape beaches and work in the surf zone are quite complicated. However, some relatively practical models are useful for understanding how beaches respond to waves from erosion or accretion. For instance, the USACE has developed a broad knowledge base, with analytical tools and predictive, numerical models for sediment management on a regional scale.

Since 2004, the USACE National Coastal Mapping Program (NCMP) has provided high-resolution elevation and imagery data along U.S. shorelines on a recurrent basis. The NCMP is executed by a Joint Airborne Lidar Bathymetry Technical Center of Expertise (JALBTCX) using its in-house survey capability called the Compact Hydrographic Airborne Rapid Survey (CHARTS) system (USACE, 2010). The CHARTS sensors include an Optech (Vaughan, Ontario, Canada) SHOALS-1000T LIDAR and an Itres Research (Calgary, Alberta, Canada) CASI-1500 hyperspectral scanner.

The SHOALS-1000 is an integrated sensor containing a 1000 pulse-*per*-second (pps) bathymetric laser, a 9000 pps topographic laser, and a digital RGB camera that records one frame every second. The CASI-1500 is a programmable hyperspectral imager capable of collecting from 4 to 288 spectral bands over a spectral range of 375 to 1050 nm, at pixel sizes from 20 cm to 5 m depending on system configuration. Bathymetric data are collected from the shoreline to 1 km offshore at 5-m spacing The RGB digital imagery have a ground resolution of 20 cm *per* pixel, and the CASI imagery have a ground resolution of 0.5 to 2 m *per* pixel, depending on the operational survey requirement. The Geographic Information System (GIS) products derived from these data include seamless bathy/topo grids, bare-earth bathy/topo grids, building footprints, shorelines, seafloor reflectance images, basic land cover classifications, and RGB and hyperspectral image mosaics (Guenter, Tomas and LaRocque, 1996; USACE, 2010).

Since the NCMP was initiated in 2004, airborne LIDAR and imagery data have been collected for more than 6500 km of shorelines on the Gulf Coast, Atlantic Coast and in the Great Lakes and connecting rivers. In support of hurricane response efforts, similar data have been collected over 3500 km of Gulf and Atlantic Coast shorelines, in Mobile Bay, the Mississippi Sound, and in Lake Pontchartrain (USACE, 2010).

The USACE has also implemented a regional, coastal morphology-change model, *Cascade,* together with a toolbox for conducting analysis and data preparation (Kraus, 2003). The *Cascade* model's domains can cover temporal and spatial scales of more than a century and hundreds of kilometers. *Cascade* computes regional longshore sand-transport rates and natural bypassing at coastal inlets and river mouths and represents both regional and local trends in morphology and transport rates. The model is used in navigation-channel and shore-protection projects and in studies of overwash, dune development, river discharges of sediment, and barrier-island breaches. Thus, *Cascade* supports coastal regional sediment management by providing quantitative, predictive capability for evaluating local and regional alternatives (Zhou, 2010).

CASE STUDIES

The following three case studies were selected to illustrate and compare the use of practical LIDAR techniques for beach profiling and coastal bathymetry. The lessons learned from these case studies should help coastal researchers and managers use these techniques for flood-zone delineation, monitoring beach-nourishment projects, and mapping changes from storms or long-term sedimentary processes along sandy coasts and shallow benthic environments. The case studies do not represent all possible uses of remote sensing for beach profiling or for studying shoreline changes, but they do present some typical problems encountered. The choice of case studies was also based on the author's personal experience.

Airborne LIDAR Hydrographic Survey of Torres Strait, Australia

In 2007, an extensive LIDAR hydrographic (Airborne LIDAR Hydrography [ALH]) survey was completed in northern Australian waters. During a period of 3 mo, an area of 5800 km^2 was surveyed in the Torres Strait and the waters of the northern Great Barrier Reef. The survey was conducted for the Australian Hydrographic Office by Tenix LADS Corp. (Melbourne, Victoria, Australia) using the Laser Airborne Depth Sounder (LADS) Mk II system. The purpose of the survey was to facilitate safe navigation by high-speed customs, fisheries, and surveillance vessels and to update nautical charts (Sinclair, 2008).

Torres Strait is a shallow body of water situated between the Coral and Arafura seas, with an unknown bathymetry in 750 km^2 of its northern part. No soundings or isobaths were displayed on the nautical charts. The area was particularly challenging because of its remoteness, shallow depths, and complicated tidal regime. The average water depth is only 5 m below datum, the range of tides exceeds 5 m, and very strong tidal streams run through the area. The seabed consists of coarse sand, and powerful hydrodynamic processes have created large *sand*-wave fields throughout the area, some of which turn dry at low water levels.

LIDAR was selected as the preferred technology because multibeam echo sounders on a surface vessel would have been too slow and expensive in this shallow area. The area presented unique technical challenges because of environmental conditions, particularly the weather and water clarity. During the winter or dry season, southeast trade winds blow continuously across the area and generate steep seas that stir up seabed sediment and increase turbidity. During the summer or wet season, when cyclones occur, heavy rainfall increases sediment discharge from rivers on the southern coast of Papua New Guinea. A turbidity management plan was developed to control these factors (Sinclair, 2008).

The LADS MK II system contains a high-power, pulsed-green laser, which, at the sea surface, had a footprint of 2.5 m in diameter, and as the beam passes through the water, it slowly diverges because of scattering. The system also includes a wide-aperture, green receiver, and a high-gain photomultiplier tube with automatic gain control. Horizontal control for the survey was based on the World Geodetic System 1984. An Ashtech GG24 GPS receiver and OmniSTAR wide-area digital GPS virtual base-station service provided real-time positions calculated from corrections received *via* satellite from Darwin and Townsville, Australia.

A total of 14 bottom-mounted tide gauges were deployed throughout the survey area for periods ranging from 30 d to 4 mo. The tide data from the gauges were downloaded and sent to the Australian Bureau of Meteorology's National Tidal Center for determination of mean sea level, analysis of harmonic constituents, and calculation of the lowest astronomical tide.

The biggest limitation to bathymetric operations was poor water clarity. Therefore, a turbidity management plan was developed. The key elements of the turbidity management plan were the timing of the survey, rate of data collection, water clarity monitoring, availability of alternative survey areas and their priorities, tidal stream management, and line spacing and redundancy. The survey was planned to occur at the end of the dry season but before the onset of the wet season. This period was predicted to have the lowest turbidity. However, during operation in the dry season, the wind increased to 30 knots from the southeast, which quickly developed a significant sea state. This caused turbidity levels to increase to the extent that some sorties had to be aborted (Sinclair, 2008).

In areas at which the operating sites were close to the survey areas, water clarity could be continuously monitored, and more frequent reconnaissance of the area by light aircraft could be conducted to confirm the optimum time for surveying. Tidal streams were weakest at neap tides. At other times, strong tidal streams created high levels of turbidity, causing operations to be aborted or diverted. In highly turbid areas, mainline sounding was planned at half the normal line spacing to provide 200% coverage of the seabed. This enabled subsequent flights to fill gaps in areas of partial coverage from earlier flights. Thus, Northern Torres Strait was successfully surveyed by LIDAR, and excellent results were achieved despite difficult environmental conditions.

LIDAR Application to Modeling Sea Level Rise at the Blackwater National Wildlife Refuge, Maryland

A good case study for demonstrating the successful application of LIDAR is the Blackwater National Wildlife Refuge Restoration Project on the eastern shore of Chesapeake Bay in Maryland. Rising sea level has led to widespread degradation of the Chesapeake Bay marshes. The Blackwater Refuge, established in 1933, includes tidal marshes, freshwater ponds, and forests and is recognized as a Wetland of International Importance by the United Nations' Ramsar Convention.

The refuge has been featured prominently in studies on the impact of sea level rise on coastal wetlands. Most notably, it has been cited by the Intergovernmental Panel on Climate Change as a key example of wetland loss attributable to rising sea level due to global warming. Studies of aerial photos taken since 1938 show an expanding area of open water in the central area of the refuge, and this open water seems to parallel the record of sea level rise during the past 60 y. The U.S. Fish and Wildlife Service (USFWS) manages the refuge to support migratory waterfowl and to preserve endangered upland species. High-marsh vegetation is critical to USFWS waterfowl management, yet a broad area, once occupied by high marsh, has decreased with rising sea level (Larsen *et al.,* 2004; NOAA, 2005).

Since 1938, 8000 acres of marsh have been lost in the refuge—a rate of nearly 130 acres (52.6 ha) *per* year. The marsh is less than 1 m above sea level, and almost all of the marsh has been breached and is being drowned. Several factors have contributed to the area's severe marsh loss, including wildlife damage (primarily geese and nutria), a rising sea level, severely altered hydrology and salinity, and an increase in wave energy associated with greater stretches of open water. Although most marshes build upward through sediment deposition, Blackwater has no source of incoming sediment because the hydraulic structure is degraded, and the sea level continues to rise (Larsen, 2004; NOAA, 2005).

Considering the most recent forecasts of sea level rise, it has become apparent that, without intervention, the entire Blackwater Refuge area will be submerged in the next century. Various engineering adjustments, such as channels, dams, housing developments, and new roads, have occurred, and an understanding of tidal characteristics could minimize the ecological impact of these changes and eliminate such problems as further erosion or a rapid change in salinity that could harm marsh species. The U.S. Geological Survey (USGS) has developed an inundation model centered on the refuge and surrounding areas. Such models require a detailed topographical map upon which to superimpose future sea-level positions.

LIDAR mapping of land and shallow water surfaces has helped solve this problem. The USGS has developed a detailed LIDAR map of the refuge area at a 30-cm contour interval . With the model, the new map enables the present marsh vegetation zones to be identified as well as predictions to be made of the location and areas of future zones on a decade-by-decade basis during the next century, at increments of about 3 cm *per* decade of sea level rise (Larsen *et al.,* 2004). Several types of multispectral imagery were also used in this study, including EO-1 images of the Blackwater National Wildlife Refuge. The EO-1 is a National Aeronautics and Space Administration (NASA) satellite that flies in formation with the Landsat ETM+ (Enhanced Thematic Mapper Plus). It carries both the multispectral Advanced Land Imager with a spatial resolution of 10 m^2 and the hyperspectral Hyperion system (30-m^2 spatial resolution).

The most recent runs of the model suggest that wetland habitat in the refuge could be sustained, but only for the next 50 y, through a combination of public and private preservation efforts, including easements and federal land acquisitions. After 50 y, this area will become open water (Larsen *et al.,* 2004).

Beach Profiling in Delaware Bay Using LIDAR

Emergency and coastal resource managers in Delaware have been early users of LIDAR technology to acquire elevation data for incorporation into state and local maps being used for flood protection and other natural hazard planning. Coastal managers also hoped that the high-detail elevation data could be used for habitat studies or vegetation identification. In 2005, a coalition of state and federal agencies contracted with the USGS and NASA to collect LIDAR data for Sussex County (one of Delaware's three counties) using NASA's EAARL LIDAR system, which is specifically designed to measure submerged topography and adjacent land elevations (Carter and Scarborough, 2010).

In 2007, the LIDAR data for the remaining two counties were collected by a commercial contractor as part of a statewide orthoimagery collection project. Because of processing problems, by the time the 2007 LIDAR was flown, state managers still did not have useable data from the 2005 flights. As a result, lessons learned were not incorporated into the second contract. Problems encountered included the incompatibility of the EAARL data and the 2007 data and that third-party quality assurance and control were not conducted, both of which delayed the availability of usable statewide LIDAR data. Having worked through all the problems, Delaware emergency managers and researchers have been able to use the data to develop statewide inundation maps, to enhance flood and storm-surge modeling, and to create an early flood-warning system.

Some of the lessons learned from the Delaware project include (1) agreeing on standards before committing to project-specific deliverables; (2) knowing the end-user's hardware and software capabilities; (3) agreeing on a common format to be used throughout the entire state; (4) ensuring that all needed data and products are contract deliverables; (5) specifying that complete and accurate metadata must accompany all the deliverables; and (6) using LIDAR data to develop tools, such as inundation maps and flood and storm-surge modeling, to help coastal managers address the impacts of climate change (Carter and Scarborough, 2010).

SUMMARY AND CONCLUSIONS

LIDAR techniques combined with a GPS make it possible to obtain accurate topographical and bathymetric maps, including shoreline positions. LIDAR surveys can produce a 10-cm vertical accuracy at spatial resolutions greater than one elevation measurement *per* square meter. This meets the requirements of many coastal research and management applications of LIDAR, including delineating flood zones, monitoring beach-nourishment projects, mapping regional changes from storms or long-term sedimentary processes along sandy coasts, and analyzing shallow, benthic environments.

LIDAR and acoustic depth sounding are the two most reliable techniques for coastal bathymetry. In LIDAR bathymetry, a laser transmitter/receiver mounted on an aircraft transmits a pulse that travels to the air–water interface, where a portion of this energy reflects back to the receiver. The remaining energy propagates through the water column and reflects off the sea bottom. The water depth is calculated from the time lapse between the surface return and the bottom return.

Optical water clarity is the most limiting factor for LIDAR depth detection; therefore, it is important to conduct the LIDAR overflights during tidal and current conditions that minimize the water turbidity from sediment resuspension and river inflow. To maximize water penetration, bathymetric LIDARs employ a blue-green laser with a typical wavelength of 530 nm to range the distance to the seabed. The LIDAR system must have a *kd* factor large enough to accommodate the water depth and water turbidity at the study site. If the depth or the water turbidity is too great, one may have to use acoustic echo-sounding techniques.

Mapping SAV and coral reefs requires high-resolution (1–4 m) imagery. Coral reef ecosystems usually exist in clear water and can be classified to show different forms of coral reef: dead coral, coral rubble, algal cover, sand lagoons, and different densities of sea grasses, *etc*. However, SAV may grow in waters that are more turbid and may thus be more difficult to map.

The USACE NCMP provides high-resolution elevation and imagery data along U.S. shorelines on a recurrent basis. The GIS products derived from these data include seamless bathy/topo grids, bare-earth bathy/topo grids, building footprints, shoreline maps, seafloor reflectance images, basic land-cover classifications, and RGB and hyperspectral image mosaics. Since the NCMP was initiated in 2004, airborne LIDAR and imagery data have been collected for more than 6500 km of shorelines on the Gulf and Atlantic coasts and the Great Lakes.

The USACE has also implemented a regional coastal morphology–change model, *Cascade,* and provided a toolbox for conducting analysis and data preparation (Kraus, 2003). The model is used in navigation channels and shore-protection projects, and studies of overwash, dune development, river sediment discharge, and barrier island breaches. Thus, *Cascade* supports coastal, regional sediment management by providing quantitative, predictive capability for evaluating local and regional alternatives.

Some valuable lessons can be learned from the case studies of projects in northern Australian waters, Chesapeake Bay, and Delaware Bay. In 2007, an extensive LIDAR hydrographic (ALH) survey was completed in northern Australian waters. During a period of 3 mo, an area of 5800 km^2 was surveyed in the Torres Strait and northern Great Barrier Reef waters. A customized turbidity-management plan was fundamental to that survey. The effects of the seasons and tides were the most important factors. The optimum time to survey the Torres Strait was during the slackening of the southeast trade winds at the end of the dry season until just before the onset of the wet season. The tidal conditions were most suitable during the latter part of each neap-tide period and were unsuitable during spring tides. Because the environmental conditions continuously changed with time and location, water clarity had to be monitored and frequent reconnaissance of the operation sites by light aircraft had to be conducted to confirm the optimum time for surveying.

The Blackwater National Wildlife Refuge Restoration Project on the eastern shore of Chesapeake Bay was chosen as the second case study to demonstrate the successful application of LIDAR . Considering the most recent forecast of sea level rise, it became apparent that, without intervention, the entire Blackwater Refuge area will be submerged in the next century. Various engineering adjustments, such as channels, dams, housing developments, and new roads have occurred, and an understanding of tidal characteristics will minimize the ecological effect of these changes and could eliminate such problems as further erosion or a rapid change in salinity that could harm marsh species. The USGS has developed an inundation model centered on the refuge and surrounding areas. Such models require a detailed topographical map upon which to superimpose future sea-level positions. LIDAR mapping of land and shallow water surfaces has helped solve this problem. The USGS has developed a detailed LIDAR map of the refuge area at a 30-cm contour interval. With the model, the new map allows the present marsh vegetation zones to be identified and facilitates prediction of the location and area of future zones on a decade-by-decade basis throughout the next century, at increments of about 3 cm *per* decade of sea level rise.

Emergency and coastal resource managers in Delaware have been early users of LIDAR technology to acquire elevation data to incorporate into state and local maps for flood protection and other natural hazards planning. Between 2005 and 2007, NASA, USGS, and commercial companies were contracted to collect LIDAR data, which were used to measure submerged topography and adjacent land elevations. Some of the lessons learned from the Delaware project include (1) agreeing on standards before committing to project-specific deliverables; (2) knowing the end-user's hardware and software capabilities; (3) agreeing on a common format to be used throughout the entire state; (4) ensuring that all needed data and products are contract deliverables; (5) specifying that complete and accurate metadata must accompany all deliverables; and (6) using LIDAR data to develop tools, such as inundation maps and flood and storm-surge modeling, to help coastal managers address the impacts of climate change.

ACKNOWLEDGMENTS

This research was supported in part by NOAA Sea Grant (NA09OAR4170070-R/ETE-15) and by the NASA Experimental Program to Stimulate Research (EPSCoR) at the University of Delaware.

LITERATURE CITED

Ackermann, F., 1999. Airborne laser scanning—present status and future expectations. *ISPRS Journal of Photogrammetry and Remote Sensing,* 54, 64–67.

Andrade, F. and Ferreira, M.A., 2006. A simple method of measuring beach profiles. *Journal of Coastal Research,* 22, 995–999.

Avery, T.E. and Berlin, G.L., 1992. *Fundamentals of Remote Sensing and Airphoto Interpretation*. New York: Macmillan Publishing Company, 472p.

Bergeron, E.; Worley, C.R., and O'Brien, T., 2007. Progress in the development of shallow water mapping systems. *Sea Technology,* 48(6), 10–15.

Boak, E.H. and Turner, I.L. 2005. Shoreline definition and detection: a review. *Journal of Coastal Research,* 21, 688–703.

Bonisteel, J.M.; Nayegandhi, A.; Brock, J.C.; Wright, C.W.; Stevens, S.; Yates, X., and Klipp, E.S., 2009a. *EAARL Coastal Topography—Assateague Island National Seashore 2008: First Surface*. Reston, Virginia: U.S. Geological Survey Data Series 446.

Bonisteel, J.M.; Nayegandhi, A.; Wright, C.W.; Brock, J.C., and Nagle, D.B., 2009b. *Experimental Advanced Airborne Research LIDAR (EAARL) Data Processing Manual*. Reston, Virginia: U.S. Geological Survey Open-File Report 2009–1078, 38p.

Brock, J. and Sallenger, A., 2000. *Airborne Topographic Mapping for Coastal Science and Resource Management*. Reston, Virginia: U.S. Geological Survey Open-File Report 01–46, 4p.

Brock, J.; Wright, C.W.; Hernandez, R., and Thompson, P., 2006. Airborne LIDAR sensing of massive stony coral colonies on patch reefs in the northern Florida reef tract. *Remote Sensing of Environment,* 104, 31–42.

Brock, J.C. and Purkis, S.J., 2009. The emerging role of LIDAR remote sensing in coastal research and resource management. *Journal of Coastal Research,* Special Issue 53, pp. 1–5.

Brock, J.C.; Wright, C.W.; Clayton, T.D., and Nayegandhi, A., 2004. LIDAR optical rugosity of coral reefs in Biscayne National Park, Florida. *Coral Reefs,* 23, 48–59.

Carter, D. and Scarborough, R., 2010. Sharing Delaware's LIDAR lessons. *In: Local Strategies for Addressing Climate Change.* Charleston, South Carolina: NOAA Coastal Services Center Report, 2, 16–17.

Chadwick, W., 2010. Remotely operated vehicles (ROVs) and autonomous underwater vehicles (AUVs). *NOAA Ocean Explorer: Submarine Ring of Fire 2002—Background*. http://oceanexplorer.noaa.gov/explorations/02fire/background/rovs_auvs/rov_auv.html (accessed January 10, 2011).

Costa, B.M.; Battista, T.A., and Pittman, S.J., 2009. Comparative evaluation of airborne LIDAR and ship-based multibeam SoNAR bathymetry and intensity for mapping coral reef ecosystems. *Remote Sensing of Environment,* 113, 1082–1100.

Cracknell, A.P. and Hayes, L., 2007. *Introduction to Remote Sensing*. New York: CRC Press.

Deronde, B.; Houthuys, R.; Debruyn, W.; Fransaer, D.; Lancker, V.V., and Hernriet, J.-P., 2006. Use of airborne hyperspectral data and Laser scan data to study beach morphodynamics along the Belgian coast. *Journal of Coastal Research,* 22, 1108–1117.

Estep, L.L.; Lillycrop, W.J., and Parson, L.E., 1994. Estimation of maximum depth of penetration of a bathymetric LIDAR system using a Secchi depth data base. *Marine Technology Society Journal,* 28, 31–36.

Finkl, C.W., 1996. What might happen to America's shorelines if artificial beach replenishment is curtailed: a prognosis for southeastern Florida and other sandy regions along regressive coasts. *Journal of Coastal Research,* 12, 2–9.

Finkl, C.W.; Benedet, L., and Andrews, J.L., 2005. Interpretation of seabed geomorphology based on spatial analysis of high-density airborne laser bathymetry (ALB). *Journal of Coastal Research,* 21, 501–514.

Gares, P.A.; Wang, Y., and White, S.A., 2006. Using LIDAR to monitor a beach nourishment project at Wrightsville Beach, North Carolina, USA. *Journal of Coastal Research,* 22, 1206–1219.

Garono, R.J.; Simenstad, C.A.; Robinson, R., and Ripley, H., 2004. Using high spatial resolution hyperspectral imagery to map intertidal habitat structure in Hood Canal Washington, USA. *Canadian Journal of Remote Sensing,* 30, 54–63.

Gesch, D.B., 2009. Analysis of Lidar elevation data for improved identification and delineation of lands vulnerable to sea-level rise. *Journal of Coastal Research*, Special Issue 53, pp. 49–58.

Guenther, G.; LaRocque, P., and Lillycrop, W., 1994. Multiple surface channels in SHOALS airborne LIDAR. *In:* Jaffe, J.S. (ed.), *Ocean Optics XII,* SPIE Proceedings Volume 2258, pp. 422–430.

Guenther, G.C.; Tomas, R.W.L., and LaRocque, P.E., 1996. Design considerations for achieving high accuracy with the SHOALS bathymetric LIDAR system. *In:* Feigels, V.I. and Kopilevich, Y.I. (eds.), *Laser Remote Sensing of Natural Waters: From Theory to Practice,* SPIE Proceedings Volume 2964, pp. 54–71.

Guenther, G., 2007. Airborne LIDAR bathymetry digital elevation: model technologies and applications: In: Maune, D. (ed.) *The DEM Users Manual,* 2nd edition. Bethesda, Maryland: American Society for Photogrammetry and Remote Sensing, pp. 253–320.

Gutierrez, R.; Gibeaut, J.C.; Crawford, M.M.; Mahoney, M.P.; Smith, S., Gutelius, W.; Carswell, D., and MacPherson, E., 1998. Airborne laser swath mapping of Galveston Island and Bolivar Peninsula, Texas. *In: Proceedings of the Fifth International Conference on Remote Sensing for Marine and Coastal Environments,* Volume 1 (San Diego, California, MTRI) 1236–1243.

Hapke, C.J., 2010. Integration of LIDAR and historical maps to measure coastal change on a variety of time and spatial scales. *In:* Wang, Y. (ed.), *Remote Sensing of Coastal Environments*. Boca Raton, Florida: CRC Press.

Irish, J.L. and Lillycrop, W.J., 1997. Monitoring New Pass, Florida, with high-density LIDAR bathymetry. *Journal of Coastal Research,* 13, 1130–1140.

Irish, J.L. and Lillycrop, W.J., 1999. Scanning laser mapping of the coastal zone: the SHOALS system. *ISPRS Journal of Photogram and Remote Sensing,* 54, 123–129.

Irish, J.L. and White, T.E., 1998. Coastal engineering applications of high resolution bathymetry. *Coastal Engineering,* 35, 47–71.

Jensen, J.R., 2007. *Remote Sensing of the Environment: An Earth Resource Perspective*. 2nd edition. Upper Saddle River, New Jersey: Prentice-Hall, 592p.

Kempeneers, P.; Deronde, B.; Provoost, S., and Houthuys, R., 2009. Synergy of airborne digital camera and LIDAR data to map coastal dune vegetation. *Journal of Coastal Research,* 53, 73–82.

Klemas, V., 2009. The role of remote sensing in predicting and determining coastal storm impacts. *Journal of Coastal Research,* 25, 1264–1275.

Krabill, W.B.; Wright, C.W.; Swift, R.N.; Frederick, E.B.; Manizade, S.S.; Yungel, J.K.; Martin, C.F.; Sonntag, J.G.; Duffy, M.; Hulslander, W., and Brock, J.C., 2000. Airborne laser mapping of Assateague National Seashore Beach. *Photogrammetric Engineering and Remote Sensing,* 66, 65–71.

Kraus, N.C., 2003. *Research Brief: Coastal Morphology-Change Models*. Vicksburg, Mississippi: USACE Engineer Research and Development Center.

Larsen, C.; Clark, I.; Guntenspergen, G.; Cahoon, D.; Caruso, V.; Hupp, C., and Yanosky, T., 2004. *The Blackwater NWR Inundation Model: Rising Sea Level on a Low-lying Coast—Land Use Planning for Wetlands*. Reston, Virginia: U.S. Geological Survey Open-File Report 04–1302.

Lee, Z.P.; Hu, C.; Casey, B.; Shang, S.; Dierssen, H., and Arnone, R., 2010. Global shallow-water bathymetry from satellite ocean color data. *EOS, Transactions, American Geophysical Union,* 91, 1–2.

Lillycrop, W.J.; Irish, J.L., and Parson, L.E., 1997. SHOALS System. *Sea Technology,* 38, 17–25.

Lillycrop, W.J.; Pope, R.W., and Wozencraft, J.M., 2002. Airborne LIDAR hydrography: a vision for tomorrow. *Sea Technology*, 43:6, 27–34.

Maeder, J.; Narumalani, S.; Rundquist, D.; Perk, R.; Schalles, J.; Hutchins, K., and Keck, J., 2002. Classifying and mapping general coral-reef structure using IKONOS data. *Photogrammetric Engineering and Remote Sensing,* 68, 1297–1305.

Mayer, L.A.; Raymond, R.; Glang, G.; Richardson, M.D.; Traykovski, P.A., and Trembanis, A.C., 2007. High resolution mapping of mines and ripples at the Martha's Vineyard Coastal Observatory. *IEEE Journal of Oceanic Engineering,* 32, 133–149.

McKean, J.; Nagel, D.; Tonina, D.; Bailey, P.; Wright, C.W.; Bohn, C., and Nayegandhi, A., 2009. Remote sensing of channels and riparian zones with a narrow-beam aquatic-terrestrial LIDAR. *Remote Sensing,* 1, 1065–096.

Mishra, D.; Narumalani, S.; Rundquist, D., and Lawson, M., 2006. Benthic habitat mapping in tropical marine environments using QuickBird multispectral data. *Photogrammetric Engineering and Remote Sensing,* 72, 1037–1048.

Morton, R.A. and Miller, T.L., 2005. *National Assessment of Shoreline Change, Part 2: Historical Shoreline Change and Associated Coastal Land Loss along the U.S. Southeast Atlantic Coast.* Reston, Virginia: U.S. Geological Survey Open-File Report 2005–1401, 14p.

Muirhead, K. and Cracknell, A.P., 1986. Review article: airborne LIDAR bathymetry. *International Journal of Remote Sensing,* 7, 597–606.

Mumby, P.J. and Edwards, A.J., 2002. Mapping marine environments with IKONOS imagery: enhanced spatial resolution can deliver greater thematic accuracy. *Remote Sensing of Environment,* 82, 248–257.

Nayegandhi, A. and Brock, J.C., 2008. Assessment of coastal vegetation habitats using LIDAR. *In:* Yang X. (ed.), *Lecture Notes in Geoinformation and Cartography—Remote Sensing and Geospatial Technologies for Coastal Ecosystem Assessment and Management,* Volume 14. New York: Springer Verlag, pp. 365–389.

Nayegandhi, A.; Brock, J.C., and Wright, C.W., 2009. Small-footprint, waveform-resolving LIDAR estimation of submerged and subcanopy topography in coastal environments. *International Journal of Remote Sensing,* 30, 861–878.

NOAA (National Oceanic and Atmospheric Administration), 2005. Blackwater Wildlife Refuge wetlands restoration project. *In: Tides and Currents Report*. Silver Spring, Maryland: National Ocean Service.

Parson, L.E.; Lillycrop, W.J.; Klein, C.J.; Ives, R.C., and Orlando, S.P., 1996. Use of LIDAR technology for collecting shallow bathymetry of Florida Bay. *Journal of Coastal Research,* 13, No.4.

Pastol, Y.; Le Roux, C., and Louvart, L., 2007. LITTO3D: a seamless digital terrain model. *International Hydrographic Review,* 8, 38–44.

Philpot, W., 2007. Estimating atmospheric transmission and surface reflectance from a glint-contaminated spectral image. *IEEE Transactions on Geoscience and Remote Sensing,* 45, 448–457.

Philpot, W.D.; Davis, C.O.; Bissett, P.; Mobley, C.D.; Kohler, D.D.; Lee, Z.; Snyder, W.A.; Steward, R.G.; Agrawal, Y.; Trowbridge, J.; Gould, R., and Arnone, R., 2004. Bottom characterization from hyperspectral image data. *Oceanography,* 17, 76–85.

Pittenger, R.F., 1989. Exploring and mapping the seafloor [map supplement]. *National Geographic,* 177(1), 622–637, January.

Purkis, S.J., 2005. A "reef-up" approach to classifying coral habitats from IKONOS imagery. *IEEE Transactions on Geoscience and Remote Sensing,* 43, 1375–1390.

Purkis, S. and Klemas, V., 2011. *Remote Sensing and Global Environmental Change*. Oxford, U.K.: Wiley-Blackwell.

Raber, G.T.; Jensen, J.R.; Hodgson, M.E.; Tullis, J.A.; Davis, B.A. and Berglund, J., 2007. Impact of Lidar nominal post-spacing on DEM accuracy and flood zone delineation. *Photogrammetric Engineering and Remote Sensing,* 73, 793–804.

Rasher, M.E. and Weaver, W., 1990. *Basic Photo Interpretation: A Comprehensive Approach to Interpretation of Vertical Aerial Photography for Natural Resource Applications*. Washington, DC: U.S. Department of Agriculture.

Sallenger, A.H., Krabill, W.B., Brock, J.C., Swift, R.N., Jansen, M., Manizade, S., Richmond, B., Hampto, M. and Eslinger, D., 1999. Airborne laser study quantifies El Niño-induced coastal change. *EOS, Transactions, American Geophysical Union,* 80, 89–93.

Sinclair, M., 2008. Airborne LIDAR hydrographic survey for homeland security. *Sea Technology,* 49(3), 15–20.

Stockdon, H.F.; Doran, K.S., and Sallenger, A.H., 2009. Extraction of LIDAR-based dune-crest elevations for use in examining the vulnerability of beaches to inundation during hurricanes. *Journal of Coastal Research,* 35, 59–65.

Stockdon, H.F.; Sallenger, A.H.; List, J.H., and Holman, R.A. 2002. Estimation of shoreline position and change using airborne topographic LIDAR data. *Journal of Coastal Research,* 18, 502–513.

Stoker, J.M.; Tyler, D.J.; Turnipseed, D.P.; Van Wilson, K.; and Oimoen, M.J., 2009. Integrating disparate Lidar datasets for a regional storm tide inundation analysis of Hurricane Katrina. *Journal of Coastal Research,* Special Issue 53, pp. 66–72.

Thieler, E.R. and Danforth, W.W., 1994. Historical shoreline mapping: improving techniques and reducing positioning errors. *Journal of Coastal Research,* 10, 539–548.

Thompson, R.L. and Schroeder, A.J., Jr., 2010. High-definition 3D tools for underwater surveying and inspection. *Sea Technology,* 51(4), 43–45.

Trembanis, A.C.; Hiller, T., and Patterson, M., 2008. Exploring coral reef sustainability. *Hydro International,* 12, 10–15.

USACE (U.S. Army Corps of Engineers), 2010. National Coastal Mapping Program. http://shoals.sam.usace.army.mil/Mapping.aspx (accessed January 10, 2011).

Wang, C-K. and Philpot, W.D., 2007. Using airborne bathymetric LIDAR to detect bottom type variation in shallow waters. *Remote Sensing of Environment,* 106, 123–135.

Wang, Y., 2010. *Remote Sensing of Coastal Environments*. Boca Raton, Florida: CRC Press, Taylor and Francis Group.

Webster, T.L.; Forbes, D.L.; Dickie, S., and Shreenan, R., 2004. Using topographic LIDAR to map flood risk from storm-surge events for Charlottetown, Prince Edward island, Canada. *Canadian Journal of Remote Sensing,* 30, 64–76.

West, G.R.; Lillycrop, W.J., and Pope, R.W., 2001. Utilization of airborne LIDAR bathymetry for rapid environmental assessment. *Sea Technology,* 42(6), 10–15.

Wilson, M.F.J.; O'Connell, B.; Brown, C.; Guinan, J.C., and Grehan, A.J., 2007. Multiscale terrain analysis of multibeam bathymetry data for habitat mapping on the continental slope. *Marine Geodesy,* 30, 3–35.

Wozencraft, J.M. and Lillycrop, W.J., 2003. Airborne coastal mapping, past, present, and future. *Journal of Coastal Research,* Special Issue 38, pp. 207–215.

Wozencraft, J.M. and Millar, D., 2005. Airborne LIDAR and integrated technologies for coastal mapping and charting. *Marine Technology Society Journal,* 39, 27–35.

Yang, X., 2009. *Lecture Notes in Geoinformation and Cartography: Remote Sensing and Geospatial Technologies for Coastal Ecosystem Assessment and Management*. Berlin, Germany: Springer-Verlag, 561p.

Zhou, G., 2010. Coastal 3D change pattern analysis using LIDAR series data. *In:* Wang, Y. (ed.), *Remote Sensing of Coastal Environments*. Boca Raton, FL: CRC Press, pp. 103–120.